ACS OMEGA

Article

Cite This: ACS Omega 2018, 3, 5131−5140

Detection of Lung Cancer: Concomitant Volatile Organic Compounds and Metabolomic Profiling of Six Cancer Cell Lines of Different Histological Origins

Zhunan Jia,[†,‡] Hui Zhang,[§] Choon Nam Ong,[*,§,∥] Abhijeet Patra,[†,‡] Yonghai Lu,[∥] Chwee Teck Lim,[‡,⊥,#] and Thirumalai Venkatesan[*,†,‡,¶,∇,○]

[†]NUSNNI-Nanocore, National University of Singapore, 5A Engineering Drive 1, 117411, Singapore

[‡]NUS Graduate School for Integrative Sciences and Engineering, National University of Singapore, 28 Medical Drive, 117456, Singapore

[§]NUS Environmental Research Institute and [#]Mechanobiology Institute, National University of Singapore, 5A Engineering Drive 1, 117411, Singapore

[∥]Saw Swee Hock School of Public Health, National University of Singapore, 12 Science Drive 2, 117549, Singapore

[⊥]Department of Biomedical Engineering, National University of Singapore, 9 Engineering Drive 1, 117575, Singapore

[¶]Department of Electrical Engineering, National University of Singapore, 4 Engineering Drive 3, 117583, Singapore

[∇]Department of Materials Science and Engineering, National University of Singapore, 9 Engineering Drive 1, 117574, Singapore

[○]Department of Physics, National University of Singapore, 2 Science Drive 3, 117551, Singapore

Supporting Information

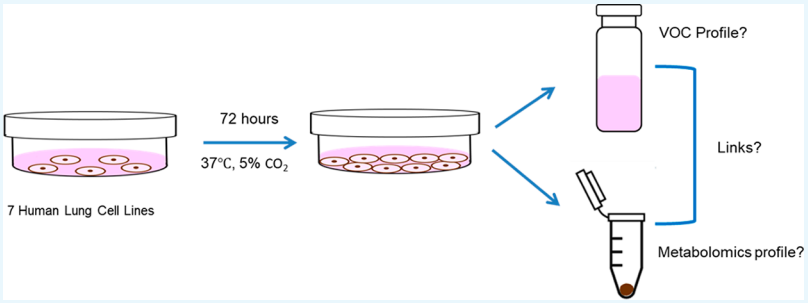

ABSTRACT: In recent years, there has been an extensive search for a non-invasive screening technique for early detection of lung cancer. Volatile organic compound (VOC) analysis in exhaled breath is one such promising technique. This approach is based on the fact that tumor growth is accompanied by unique oncogenesis, leading to detectable changes in VOC emitting profile. Here, we conducted a comprehensive profiling of VOCs and metabolites from six different lung cancer cell lines and one normal lung cell line using mass spectrometry. The concomitant VOCs and metabolite profiling allowed significant discrimination between lung cancer and normal cell, nonsmall cell lung cancer (NSCLC) and small cell lung cancer (SCLC), as well as between different subtypes of NSCLC. It was found that a combination of benzaldehyde, 2-ethylhexanol, and 2,4-decadien-1-ol could serve as potential volatile biomarkers for lung cancer. A detailed correlation between nonvolatile metabolites and VOCs can demonstrate possible biochemical pathways for VOC production by the cancer cells, thus enabling further optimization of VOCs as biomarkers. These findings could eventually lead to noninvasive early detection of lung cancer and differential diagnosis of lung cancer subtypes, thus revolutionizing lung cancer treatment.

INTRODUCTION

Lung cancer is the leading cause of cancer-related deaths globally claiming 1.59 million lives annually.[1] It is typically silent in its early stages as a result of which 84% of the cases are diagnosed in later stages (3 or 4) when treatment is ineffective and can no longer provide a cure.[2] The five year survival rate increases dramatically from 10 to 80% if the disease is discovered at stage 1.[3] Therefore, the holy grail of lung cancer treatment is early detection.

Exhaled breath volatile organic compound (VOC) analysis is one promising technique for the noninvasive early detection of lung cancer. Human breath is a complex mixture of inorganic compounds (mainly nitrogen, oxygen, and carbon dioxide) as well as more than 500 VOCs.[4,5] These VOCs that exist in parts per billion or even parts per trillion levels are produced by cell

Received: December 20, 2017
Accepted: April 5, 2018
Published: May 10, 2018

DOI: 10.1021/acsomega.7b02035
ACS Omega 2018, 3, 5131−5140

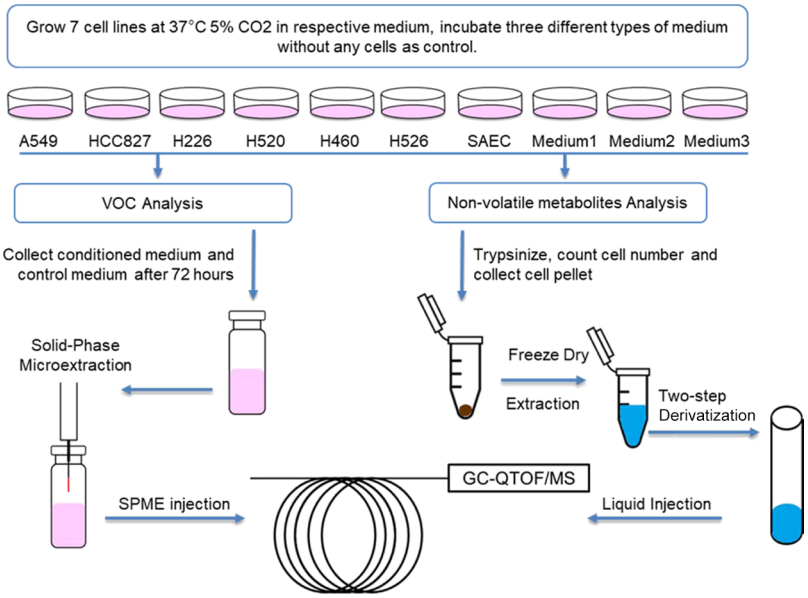

Figure 1. Schematic diagram of experimental procedures.

metabolism and exhaled into breath through blood gas exchange in the alveoli. It is well-known that several biochemical pathways are altered in lung cancer patients;[6−8] thus, it is logical to expect that they would have a different breath VOC profile with respect to healthy subjects. It has been four decades since Linus Pauling first identified more than 200 VOCs in human breath using gas chromatography mass spectrometry (GC-MS),[8] and many studies have been directed toward identification of breath VOCs associated with lung cancer.[9−12] However, until now, no consistent list of breath biomarkers for lung cancer has been generated and translated to clinical practice. This is partly because breath VOC profile is affected by many confounding factors such as environmental background, age, gender, diet, medication, smoking history, lifestyle of the individual, and so on. Prior to its use for clinical diagnosis, one effective method of investigating biomarkers associated with lung cancer while bypassing these factors is the study of VOC profiles in the headspace of in vitro lung cancer cell cultures.[13]

Lung cancer cell is classified into four major histological types: adenocarcinoma, squamous cell carcinoma, small cell carcinoma, and large cell carcinoma. Adenocarcinoma arises from epithelial cells that secrete substances into the ducts or cavities that they line. Squamous cell carcinomas are from the epithelial cells, which serve largely to seal the cavity or channel that they line (to protect the underlying cell populations). Small cell lung carcinomas (whose origin is still unknown) secrete biologically active peptides. Large cell carcinoma is a diagnosis of exclusion, indicating that the cells lack microscopic evidence of all the other histology types.[14] The prognosis and treatment options are critically dependent on the histology of the cancer: chemotherapy and radiation therapy are usually used for small cell lung cancer (SCLC) because of its sensitivity to these therapies, while surgery is performed on most of the non-SCLC (NSCLC) patients.[15] For NSCLC patients, the treatment approach also depends on the subhistology.[16] Current method to identify cancer types in the clinic involves the invasive and painful procedure of biopsy. The accuracy is often limited by the small size of the nodule and ease of access, especially in its early stages.[17] Therefore, an accurate and noninvasive test that could classify lung cancers would be very valuable for prognosis. Several studies have investigated VOC profiles from lung cancer cell culture;[18−23] however, most of these studies involved only one or two cell lines. Because of the heterogeneity of lung cancer, cell lines from different histological origins should be investigated for more accurate results. So far, few studies have profiled VOCs from different types of lung cancer cell lines, and the biochemical origins of these VOCs remain largely unknown.[24]

In this study, we cultured six different types of lung cancer cell lines (two adenocarcinomas, two squamous cell carcinomas, one large cell carcinoma, and one small cell carcinoma) and one normal small airway epithelial cell (SAEC) and investigated the VOC profile and nonvolatile metabolite profile using GC quadrupole time of flight/MS (GC-Q-TOF/MS). Figure 1 shows a schematic diagram of experimental procedures. The primary objective is to characterize the volatile and metabolic profiles of various types of lung cancer cells to provide a deeper insight for differentiating metabolic phenotypes that can be used to distinguish lung cancer cells and normal cells. On a secondary level, we aim to find the specific VOCs that can distinguish between different types of lung cancers, such as NSCLC and SCLC, as well as between subhistologies within NSCLC. In addition, the metabolites inside the cells were also profiled to find possible links between VOCs and metabolites.

RESULTS

Data Quality and Compound Identification. To simulate the natural diversity of lung cancer, six different cell lines that cover different histologies and a normal epithelia cell line as control were studied. Earlier studies had studied different types of cells cultured in Dulbecco's modified Eagle media (DMEM) to get the same VOC background.[25−27] Here, we used strictly supplier recommended medium for each cell line to ensure cells are in healthy condition. Microscopic pictures of seven cell lines grown in a supplier recommended medium are shown in Figure S1. To obtain reliable data, we used pooled quality control (QC) samples to monitor the stability of the GC-MS instrument during the entire

DOI: 10.1021/acsomega.7b02035
ACS Omega 2018, 3, 5131−5140

Table 1. Trends of VOCs in Different Cell Lines, Compared to Their Respective Medium Control[a]

		adenocarcinoma		squamous carcinoma		large-cell carcinoma	small-cell carcinoma	normal epithelial
category	VOC/cell line	A549	HCC827	H226	H520	H460	H526	SAEC
alcohol	2,4-decadien-1-ol	↑*	↑**	↑**	↑**	↑*		
	2-ethyl-1-hexanol	↑*	↑**	↑**	↑**	↑*		
	cyclohexanol	↑*	↑**	↑**	↑**		↑**	
	2-butanol					↑*		
ketone and aldehydes	acetone					↑*		↑*
	propanal	↑*	↑*		↑*	↑*	↑*	↑*
	hexanal				↓*		↓*	↓*
	nonanal						↓*	
hydrocarbons	pentane, 2-methyl	↑*	↑**	↑*	↑**	↑*	↑**	
	2-pentene, 2,4-dimethyl-						↑**	↑*
benzene derivatives	1,2,4-trimethylbenzene		↑**	↑**	↑**		↑**	
	styrene	↓*	↓**	↓**	↓**	↓*	↓**	
	toluene		↑*	↑*	↑**		↑**	
	naphthalene			↑**				
	benzaldehyde	↑*			↓**	↑*		↓*
	ethylbenzene	↓*	↓**	↓**	↓**	↓*		
	m & *p*-xylene	↓*	↓*		↓*	↓*	↑**	
	o-xylene	↓*	↓*		↓*	↓*	↑**	
	benzene, 1,3-bis(1,1-dimethylethyl)-			↓*		↓*	↑**	
	phenol, 2,4-bis(1,1-dimethylethyl)-						↑**	

[a](↑: increased in cell compared to medium; ↓: decreased in cell compared to medium; *$P < 0.05$; **$P < 0.01$).

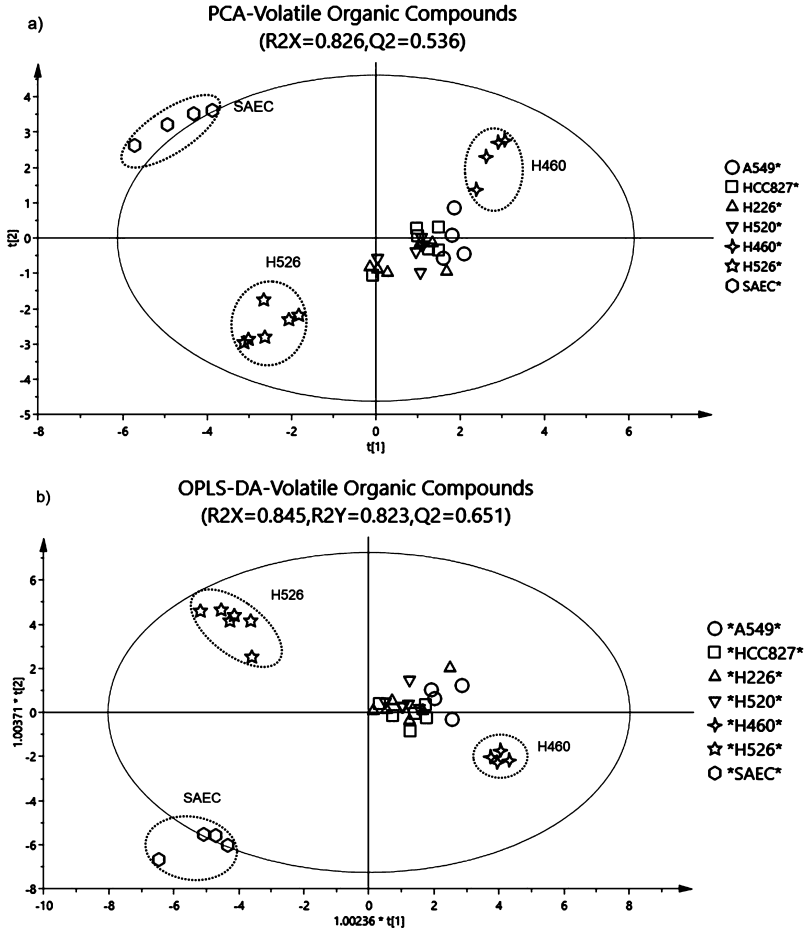

Figure 2. (a) PCA score plot of VOCs (principle components 1 and 2 explain 39.2 and 22.4% of total data variance, respectively). (b) OPLS-DA score plot of VOCs.

DOI: 10.1021/acsomega.7b02035
ACS Omega 2018, 3, 5131−5140

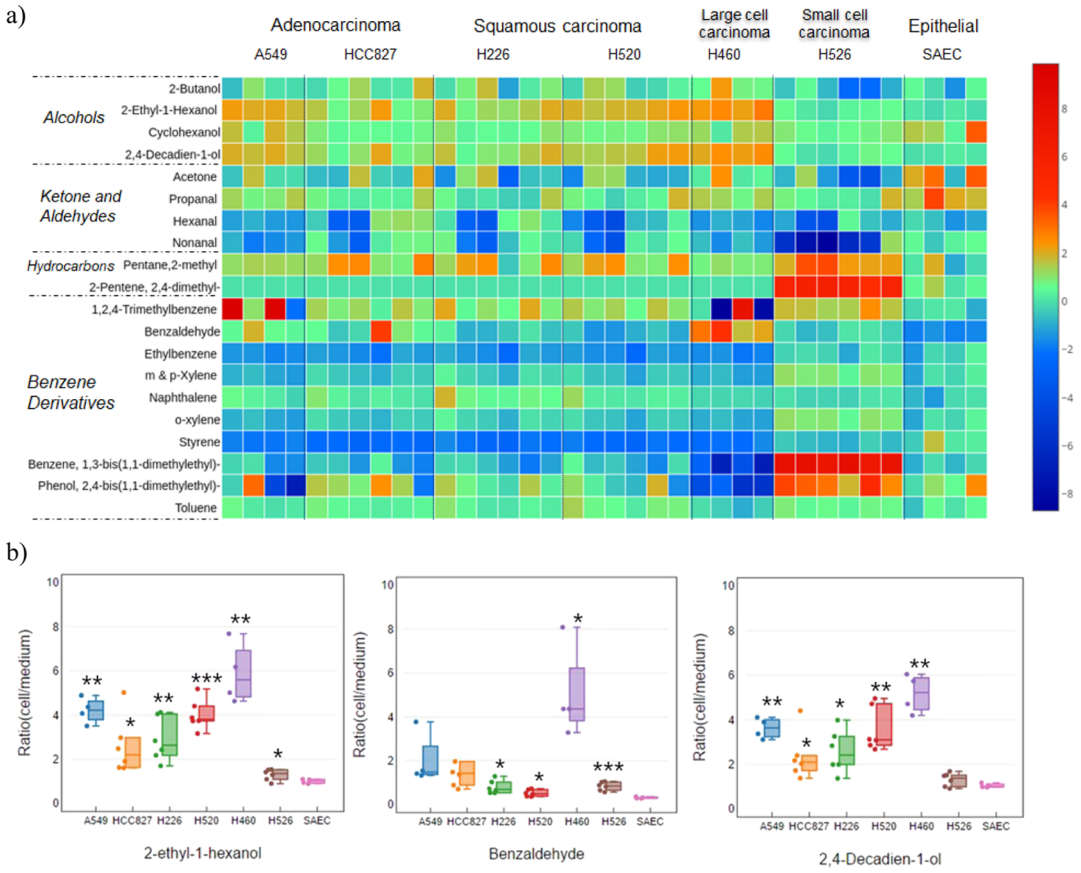

Figure 3. (a) Color-coded map of the ratio between each cell line and its medium control. The ratio is log 2-transformed. (b) Box plot of fold change of three most significantly different VOCs. Asterisks indicate the level of significance of each group compared to SAEC (*$p < 0.05$, **$p < 0.01$, ***$p < 0.001$).

experimental period. It was found that QC samples clustered together in principle component analysis (PCA) score plots in a metabolic profiling experiment with high R2 and Q2 values (Figure S2). A total ion chromatogram (TIC) of blank solid-phase microextraction (SPME) fiber is shown in Figure S3. Retention time, m/z, CAS number, and match score of the compounds identified in the blank sample were listed. For compound identification, only metabolite features with relative standard deviations below 30% were used. After performing a series of data analyses (described in Materials and Methods section), 20 differential VOCs were identified and confirmed with NIST library with a match and reverse match score of more than 700. Among them, 13 were further confirmed with analytical standards. In the metabolic profiling experiment, 37 metabolites were identified and confirmed with NIST library with a match and reverse match score of more than 700. Twenty of them were confirmed with pure analytical standards. A list of 20 VOCs is shown in Table S1. Comparison of match score of the 13 VOCs confirmed with standards is shown in Table S2. A list of 37 nonvolatile metabolites is shown in Table S3. Table S4 shows the comparison of match score of the 20 metabolites confirmed with standards. Examples of TIC for VOCs and metabolites are shown in Figures S4 and S5, respectively. Each TIC is labeled with the compounds identified. For those compounds that have been confirmed with standards, a parallel comparison of the spectrum in sample and standard is shown in Figure S6 for VOCs and Figure S7 for nonvolatile metabolites.

VOC Profiling. Before comparing VOC profile across different cell lines, the trend of VOCs in each cell line compared with its respective medium control was analyzed and shown in Table 1. Significant differences were observed between the VOC profiles from cancer cells and their respective medium controls; in contrast, normal lung epithelial cells caused fewer changes to their medium VOC component. In general, lung cancer cells emit more alcohols (2-ethyl-1-hexanol, 2,4-decadien-1-ol, and cyclohexanol), whereas there is no significant change in normal SAECs compared to its medium. 2-Methyl pentane was found to increase significantly in all cancer cells but not in SAECs. Most of the benzene derivatives decreased in the NSCLC cell, in contrast to the increase in SCLC cells. Meanwhile, there was no significant change in SAECs.

For comparison across different cell lines, a correction of the VOC concentrations due to different growth medium was performed. Specifically, the fold change of concentration of each VOC from cell to that from its medium control was calculated. PCA and orthogonal projections to latent structures-discriminant analysis (OPLS-DA) plot using identified features showed clear separation between cancer cells and normal cells (Figure 2). The plot also demonstrated that SCLC was distinct from NSCLC. Within NSCLC, large cell carcinoma was noted to be clearly separated from the rest. However, there was overlap between adenocarcinoma and squamous carcinoma cells. The high R2X, R2Y, and Q2 values indicate the validity of the PCA and OPLS-DA model. To better illustrate the degree of increase or decrease in the VOCs, the fold change of each

DOI: 10.1021/acsomega.7b02035
ACS Omega 2018, 3, 5131−5140

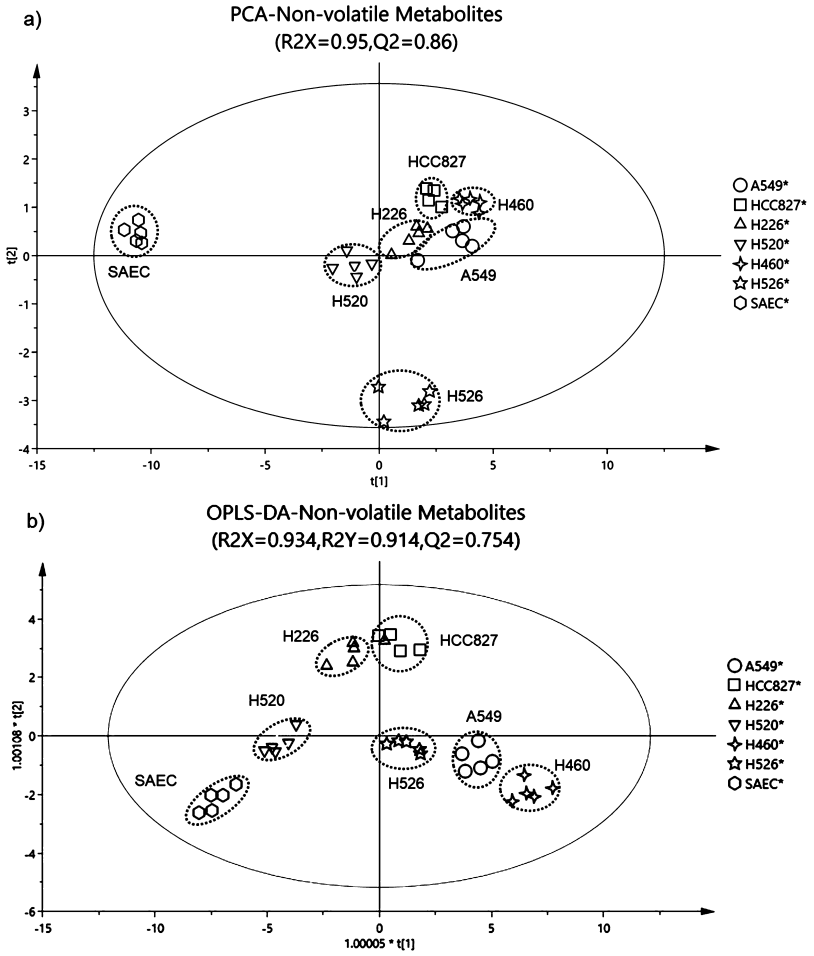

Figure 4. (a) PCA score plot of nonvolatile metabolites (principle components 1 and 2 explain 79.6 and 6.5% of total data variance, respectively). (b) OPLS-DA score plot of nonvolatile metabolites.

VOC in the cell to that in the medium control was calculated, log 2-transformed, and then plotted in the color-coded map and shown in Figure 3a. Positive values indicate emission of the VOC, whereas negative values indicate consumption from the medium. To further identify the VOCs that can be used to distinguish cancer cells versus normal cells, NSCLC versus SCLC, as well as large cell carcinoma versus other NSCLC, receiver operating characteristic (ROC) analysis was performed between these groups. Figure S3 shows the ROC curve of VOCs with area under curve (AUC) values of more than 0.9 in each analysis. The VOCs that distinguish cancer versus noncancer and large cell versus other NSCLC were found to be the same: 2-ethyl-1-hexanol, 2,4-decadien-1-ol, and benzaldehyde. Figure 3b shows a box plot of fold change of these three VOCs.

Metabolite Profiling. We further investigated the nonvolatile metabolite profile of the seven cell lines. PCA and OPLS-DA analysis showed clear distinct clusters of the seven types of cell lines with high R2X, R2Y, and Q2 values (Figure 4). The relative concentration of each metabolite was linearly normalized into the range of −1 to 1 and plotted in the heat map shown in Figure 5a. Higher value represents higher relative concentration and vice versa. To better reveal the difference of various classes of metabolites between different cell lines, a box plot of the sum of the concentration of the amino acids, carbohydrates, lipids, and nucleotides is shown in Figure 5b.

DISCUSSION

In-depth and comprehensive characterization of tumor phenotypes will lead to early diagnosis and therapeutic strategies. Recently, metabolomics have been extensively used to identify the biomarkers of various diseases. The application to cancer study is beneficial because it reflects the biochemical compositions of cancer-type-specific pathophysiological processes. Studying the VOC and metabolic profile of in vitro cancer cells provides an elegant alternative to non-invasive cancer diagnostics and bypass many confounding factors associated with human samples. However, its application is limited by a lack of validated cancer biomarkers and the largely unknown origins of VOCs. Here, we analyzed the VOCs in the headspace and the intracellular metabolites from six different lung cancer cell lines and one normal lung epithelial cell line as control. We aim to find differential VOCs and metabolites that can discriminate between cancer and normal cells, as well as between different subtypes of lung cancer. By linking the metabolites and VOC profiles, we also investigate the possible biochemical origins of VOCs.

VOC and Metabolite Differences between Lung Cancer and Noncancerous Cells. 2-Methyl pentane increased significantly in all types of cancer cells with respect to the medium, but there was no significant change in the case of SAEC. In previous studies, 2-methyl pentane was found to have increased in lung adenocarcinoma NCI-H2087.[21] Higher concentration of 2-methyl pentane was also reported in

DOI: 10.1021/acsomega.7b02035
ACS Omega 2018, 3, 5131−5140

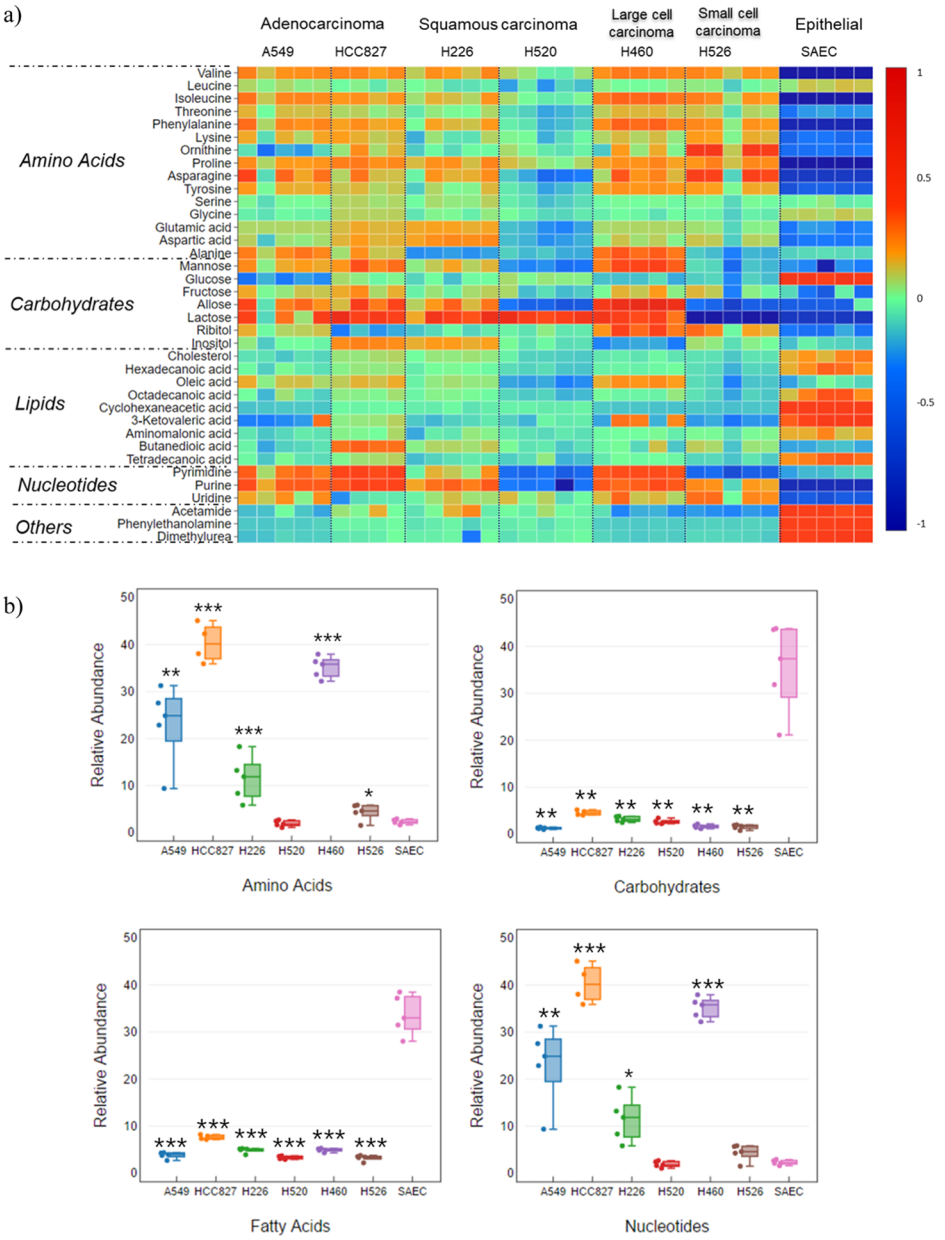

Figure 5. (a) Color-coded map of nonvolatile metabolites. (b) Comparison of amino acids, carbohydrates, fatty acids, and nucleotides in lung cell lines. Asterisks indicate the level of significance of each group compared to SAEC (*p < 0.05, **p < 0.01, ***p < 0.001).

NSCLC patients' breath,[28−30] The main mechanism that affects the emission of alkanes is oxidative stress. Alkanes are mainly produced by the peroxidation of polyunsaturated fatty acids by reactive oxygen species,[31,32] via lipid peroxidation. Hence, the increased level of 2-methyl pentane in cancer cells reflects the increased level of oxidative stress in cancer cells. 2-Ethyl-1-hexanol and 2,4-decadien-1-ol increased significantly in all three types of NSCLCs. However, the level of these two alcohols increased only slightly in SCLCs and did not change at all in SAECs. A significant increase in 2-ethyl-1-hexanol has been observed from lung adenocarcinoma.[21,33] Study on lung cancer patients' breath also revealed a higher concentration of 2-ethyl-1-hexanol than in healthy control.[34] 2-Ethyl-1-hexanol was also found exclusively in lung cancer patients' saliva samples but not in other cancer patients' saliva.[35] It was postulated that alcohols are produced by the oxidation of alkanes by cytochrome p450 (CYP450), a group of enzymes that are over-activated in lung cancer tissue.[32] As alkanes result from lipid peroxidation resulting from oxidative stress, the increased level of these two alcohols could be the result of increased oxidative stress and upregulated CYP450.

At the cellular metabolite level, significant differences were observed between cancer cells and normal epithelial cells. The most conspicuous difference was at the glucose level. As described by the famous "Warburg effect", a major hallmark of cancer cells is their high rate of glycolysis even in aerobic conditions to meet their high energy expenditure.[36] Our results showed that glucose was much lower in all cancer cells, which suggest the rapid consumption of glucose through glycolysis. Amino acids are the building blocks of proteins and are essential for cell proliferation.[37] Our results showed that amino acids were about threefold higher in cancer cells than in SAECs, except for H520, in which comparable lower levels of amino acids were observed. The accumulation of amino acids could be

DOI: 10.1021/acsomega.7b02035
ACS Omega 2018, 3, 5131−5140

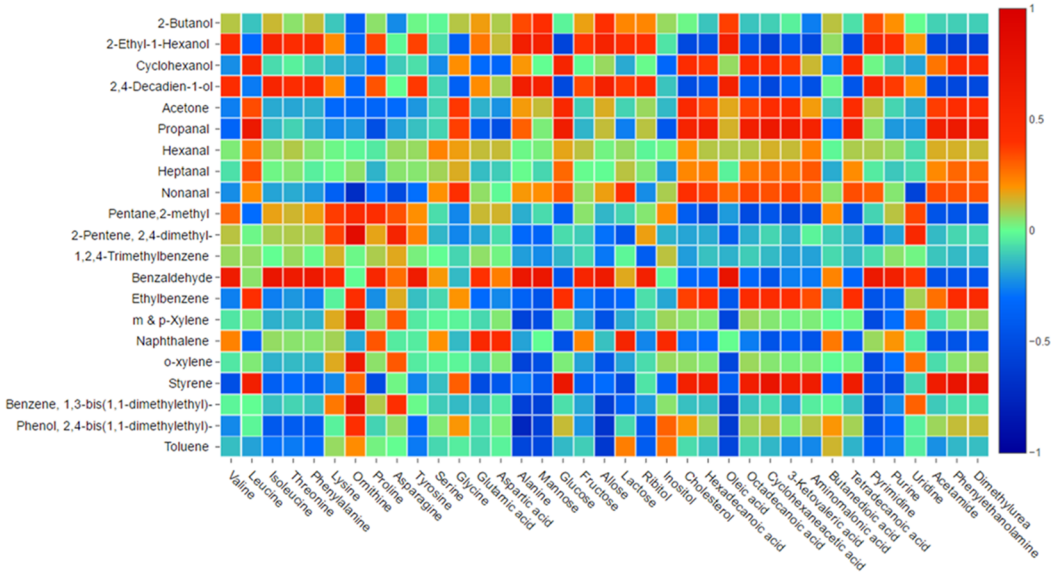

Figure 6. Pearson's correlation between VOCs and nonvolatile metabolites.

attributed to the increased uptake by cancer cells because of the increase in protein synthesis as well as energy consumption. Glutamine is a critical source of energy for cancer cells and also a nitrogen donor for the synthesis of other amino acids. Asparagine was found to regulate the uptake of other amino acids such as serine, arginine, and histidine. It is also involved in coordinating nucleotide synthesis.[38] The accumulated evidence also suggests that tumors preferentially uptake branched-chain amino acids such as leucine, isoleucine, and valine because they are essential nutrients for cancer growth and are used as a source of energy.[39] Tang et al. studied the coexpression pattern of tyrosine-protein kinase (MET) and epidermal growth factor receptor (EGFR) in 11 lung cancer cell lines, including A549, H226, and H520.[40] It was found that H520 is MET-negative/EGFR-negative, whereas A549 and H226 have strong expression of both genes. Both of these two genes encode receptors that regulate many physiological processes including proliferation. This could explain the fact that H520 has much lower levels of amino acids than all the other lung cancer cell lines.

Fatty acids are used for both structural and functional purposes. It was reported that β-oxidation of fatty acids is an important source of energy production in cancer cells.[41] This is also consistent with our results where lower levels of fatty acids were observed in cancer cells. Nucleotides are required for many biological processes in all cells. During cell proliferation, increased nucleotide synthesis is essential for DNA replication and RNA production.[39] Higher levels of nucleotides in cancer cells observed in our study confirm this.

VOC Profile of Different Histological Types of Lung Cancer. ROC analysis revealed that SCLC can be distinguished from NSCLC by *m*- and *p*-xylenes, ethylbenzene, styrene, *o*-xylene, 1,3-bis(1,1-dimethylethyl)-benzene, and 2,4-bis(1,1-dimethylethyl)-phenol; each of these VOCs has AUC values higher than 0.95. SCLC occurs almost exclusively in smokers, whereas NSCLC occurs in both smokers and nonsmokers.[42−44] Increased levels of benzene derivatives might reflect the smoking habits of the donor from which the cell line was established.

2,4-Decadien-1-ol, 2-ethyl-1-hexanol, and benzaldehyde are the key compounds differentiating the large cell carcinoma level of these three VOCs that are higher in large cell carcinoma than in adenocarcinoma and squamous cell carcinoma. Benzaldehyde was previously found to be decreased in cell lines with squamous cell carcinoma histology as compared with adenocarcinomas cells.[24] In our study, a similar trend was observed. The level of benzaldehyde was the highest in large cell carcinoma, followed by adenocarcinoma and then by squamous carcinoma. Benzaldehyde in human breath was postulated to be related to environmental factors;[45] its origin in cells is still unknown.

Links between VOCs and Metabolites. To reveal the links between VOCs and cellular metabolites, a Pearson's correlation test was performed; the correlation coefficient is shown in Figure 6. The level of 2-methyl pentane is negatively correlated with the levels of all detected fatty acids (except for butanedioic acid). Cancer cells have lower levels of intracellular fatty acids but higher level of 2-methyl pentane. This is consistent with the postulation that oxidation of fatty acids results in alkanes as a volatile byproduct.[31,32] Levels of 2-ethyl-1-hexanol and 2,4-decadien-1-ol were strongly negatively correlated with the levels of three amino acids (leucine, ornithine, and glycine), glucose, cholesterol, as well as many fatty acid molecules (hexadecanoic acid, octadecanoic acid, cyclohexaneacetic acid, 3-ketovaleric acid, aminomalonic acid, and tetradecanoic acid). This suggested that the production of these two alcohols may be associated with multiple cellular metabolism pathways. Benzaldehyde has a strong negative correlation with glucose, cholesterol, and several fatty acid molecules. Levels of propanal and nonanal are negatively correlated with most amino acids identified. Cancer cells have lower levels of propanal and nonanal but higher levels of amino acids. This suggests that these two aldehydes could be the precursors in amino acid anabolism pathways. The exact biochemical pathways for VOCs are largely unknown. It has been postulated that alkanes are produced from the peroxidation of lipids, and they will be further oxidized into alcohols by P450, which can be further oxidized into aldehydes and carboxylic acids by alcohol dehydrogenase and aldehyde dehydrogenese, respectively.[31,32] Here, we observed higher levels of alkane and lower levels of fatty acids in cancer cells. The increased level of two hydrocarbons is likely due to the fast

DOI: 10.1021/acsomega.7b02035
ACS Omega 2018, 3, 5131−5140

oxidation of fatty acids in cancer cells. We also observed increased level of several alcohols in cancer cells which could be due to the increased level of P450, oxidizing alkanes into alcohols. However, observations from the current study are correlative only; further studies are needed to identify the exact biochemical pathway for each specific VOC.

CONCLUSIONS

In this study, we conducted a comprehensive profiling of VOCs emitted by different cell lines and also their respective nonvolatile cellular metabolites by using GC-Q-TOF-MS. Both the VOC and cellular metabolite profiles allowed significant discrimination between lung cancer and normal epithelial cells. The data demonstrated that cellular metabolite profiles also allowed discrimination between each specific cell lines. Using VOC profile, we were able to discriminate small cell carcinoma from nonsmall cell carcinoma; within nonsmall cell carcinoma, large cell carcinoma has a distinct VOC profile. A correlation test also reveals possible biochemical pathways of VOCs. These findings could eventually lead to early noninvasive screening for lung cancer as well as differential diagnosis of different histological types of lung cancer, thus saving millions of lives and reducing healthcare cost dramatically.

MATERIALS AND METHODS

Human Lung Cell Culture. Seven human lung cell lines were used: lung adenocarcinoma A549, lung large cell carcinoma H460 (kindly provided by Prof Shen Han-Ming, Department of Physiology, National University of Singapore), SAEC (kindly provided by Prof Bay Boon Huat, Department of Anatomy, National University of Singapore), lung squamous carcinoma H520, H226, lung adenocarcinoma HCC827, and lung small cell carcinoma H526 were purchased from ATCC, United States. Cell lines have been propagated using the formulation suggested by ATCC. A549 was cultured in DMEM high-glucose medium supplemented with 10% fetal bovine serum. H460, H226, H520, HCC827, H526, and MRC5 were cultured in RPMI-1640 medium supplemented with 10% fetal bovine serum. The human SAEC was cultured in SAGM (Lonza, Singapore). All cell lines were cultured under standard conditions at 37 °C in humidified atmosphere in 5% CO_2. One million of each cell line was cultured in 12 mL of respective medium in Petri dish with a diameter of 10 cm. After 72 h of growth, the conditioned medium was collected into 20 mL headspace vials, three types of growth medium without any cells were cultured under the same condition as control groups for VOC profiling. For metabolite profiling, the cells were trypsinized, counted with a hemocytometer, washed with phosphate-buffered saline once, autoclaved with DI water once, and then frozen at −80 °C for further processing. All the cell line samples and control samples were prepared in 4−6 replicates.

Reagents and Analytical Standards. *N*-Methyl-*N*-(trimethylsilyl)-trifluoroacetamide (MSTFA), methoxy-amine hydrochloride, FOMC-glycine, and pyridine were obtained from Sigma-Aldrich. A liquid mixture of 53 VOC standards was purchased from AccuStandard. Twelve VOC standards were purchased from Sigma-Aldrich, including 2-methyl pentane, pentane, 2-butanone, isoprene, acetaldehyde, propanal, pentanal, hexanal, heptanal, octanal, monanal, and 2-ethyl-1-hexanol. Twenty nonvolatile metabolite standards were purchased from Sigma-Aldrich. VOC standards and metabolite standards were diluted and measured using the same methods for measuring samples.

VOC Profiling: SPME and GC-Q-TOF/MS Conditions. A medium (5 mL) was sealed in a 20 mL headspace vial (Agilent Technologies, Singapore) with a polytetrafluoroethylene/silicone crimp seal and stored at 4 °C until analysis. The fiber used was 50/30 μm Carboxen/DVB/PDMS, Stableflex, 24 Ga (Agilent Technologies, Singapore). A new fiber was conditioned at 270 °C for 1 h before use. Before running each sample, the fiber was conditioned at 250 °C for 10 min. Sample vials were incubated on a PAL autosampler in incubation module at 40 °C for 30 min. The extraction time is 20 min, and the desorption time is 30 s.

The analysis of VOCs on the SPME fiber was performed with an Agilent 7890A gas chromatograph with 7200 quadrupole time-of-flight mass spectrometer (GC-Q-TOF/MS). The separation was performed on a DB-5MS capillary column, 30 m length × 0.25 mm i.d. × 0.25 μm thickness, and conducted in splitless modes using ultrahigh-purity helium as the carrier gas with a flow rate of 1 mL/min. The oven temperature was held at 40 °C for 4 min, increased by 5 °C/min to 100 °C, increased at 10 °C/min to 120 °C, increased at 20 °C/min to 300 °C, and finally held at this temperature for 6 min; the total run time was 33 min. The injection port was held at 250 °C. The injection mode is splitless. The ion source was operated in an electron ionization mode, and its temperature was 230 °C. The mass scan range for TOF was from m/z 20 to 500. Mass calibration was conducted for every six samples to maintain high mass accuracy. One QC sample was run every six samples to evaluate instrument stability.

Metabolite Profiling: Sample Preparation and GC-Q-TOF/MS Conditions. The sample preparation protocol was adopted from previous studies.[46,47] The cell pellet was freeze-dried overnight. Methanol (500 μL) and water (4:1, v/v) containing 25 μg/mL of FMOC-glycine as the internal standard were added to each cell pellet sample for metabolite extraction. The samples were then homogenized for 10 min at 25 Hz in TissueLyser (Qiagen, USA). The samples were then sonicated for 10 min in an ice water bath to improve the extraction efficiency. Followed by sonication, the samples were centrifuged at 14 000 rpm at 4 °C for 10 min. The supernatant was collected and 20 μL was used for derivatization and GC/MS. For derivatization, 20 μL of the sample was transferred into a glass shell vial and dried in a CentriVap concentrator (Labconco, USA). Two steps of derivatization were carried out first with 100 μL of methoxyamine in pyridine (5 mg/mL) at 60 °C for 2 h and second with 100 μL of MSTFA at 37 °C for 16 hours. After derivatization, the samples were transferred to a GC vial and run within the same day. 20 μL was taken out from each sample to form a pooled QC sample and then split into seven QC samples.

For GC-MS analysis, an Agilent 7890A gas chromatograph with 7200 quadrupole time-of-flight mass spectrometer (GC-Q-TOF/MS) was used. The separation was performed on a DB-5MS capillary column, 30 m length × 0.25 mm i.d. × 0.25 μm thickness, and conducted in splitess modes using ultra-high purity helium as a carrier gas with a flow rate of 1 mL/min. The injection volume was 1 μL. The oven temperature was held at 90 °C for 1 min and increased by 20 °C/min to 130 °C, increased at 6 °C/min to 280 °C, and then increased at 25 °C/min to 300 °C, the latter temperature was held for 6 min, and the total run time was 34.8 min. The solvent cut time was 4.5

DOI: 10.1021/acsomega.7b02035
ACS Omega 2018, 3, 5131−5140

min. The ion source was operated in an electron ionization mode, and its temperature was 230 °C. The mass scan range for TOF was from m/z 50 to 800. Mass calibration was conducted for every six samples to maintain high mass accuracy. One QC sample was run every six samples to evaluate the instrument stability.

Data Analysis. *Raw Data Analysis.* The raw chromatogram data from GC/MS were first transformed to mzData files in MassHunter Qualitative analysis software (Agilent) and then exported to Mzmine software for feature detection and alignment. The aligned features were normalized through QC samples for VOC profiling and through internal standards and cell number for metabolite profiling. The features were then screened using two criteria: relative standard deviation ≤ 30% and detection frequency ≥ 6/6. PCA and OPLS-DA were performed in SIMCA-P. Kruskal–Wallis test for comparison between more than two groups was performed using Multi Experiment Viewer software. The features with variable importance in project scores above 1 in the OPLS-DA model and p-value less than 0.05 in the Kruskal–Wallis test were considered to be statistically significant. The heat map was plotted using Plotly.

Metabolite Identification. The metabolites were identified on the basis of mass spectra and accurate mass fragments by searching NIST 11 library; only compounds with a match and reverse match score of more than 700 were reported. Thirteen VOC standards and 20 metabolite standards (as mentioned in Materials and Methods section) were analyzed through the same respective GC-MS methods to confirm the retention time and mass spectrum of each compound.

■ ASSOCIATED CONTENT

Supporting Information

The Supporting Information is available free of charge on the ACS Publications website at DOI: 10.1021/acsomega.7b02035.

m/z, CAS number, and retention time of 20 statistically differential VOCs; comparison of match, reverse match, and probability scores of the 13 VOCs confirmed with standards; retention time and m/z values of 37 statistically differential nonvolatile metabolites; comparison of match, reverse match, and probability scores of the 20 nonvolatile metabolites confirmed with standards; morphology of eight lung cell lines when cultured in a supplier recommended medium; PCA score plot of metabolite profiling showing QC samples clustered together; features detected in the blank SPME fiber; TIC of 20 VOCs in representative samples; TIC of 37 nonvolatile metabolites in representative samples; parallel comparison of spectra of 13 VOCs in sample and in standards); parallel comparison of spectra of 20 nonvolatile metabolites in sample and in standards; ROC analysis of (a) cancer versus normal cell, (b) large cell versus other NSCLC, and (c) SCLC versus NSCLC (PDF)

■ AUTHOR INFORMATION

Corresponding Authors

*E-mail: ephocn@nus.edu.sg (C.N.O.).
*E-mail: venky@nus.edu.sg (T.V.).

ORCID

Choon Nam Ong: 0000-0002-4002-1725
Abhijeet Patra: 0000-0003-0422-3319
Chwee Teck Lim: 0000-0003-4019-9782

Author Contributions

Conceptualization, Z.J., T.V., and C.O.; method, Z.J. and H.Z.; data analysis, Z.J., H.Z. and Y.L.; writing-first draft, Z.J. and C.O.; writing-reviewing and editing, Z.J., C.O., T.V., C.L. and A.P.

Notes

The authors declare no competing financial interest.

■ ACKNOWLEDGMENTS

The authors gratefully acknowledge Shen Hanh Ming and Bay Boon Huat for the cell lines, Ren yi, Ng Cheng Teng and Viknish Krishnan-Kutty for helpful guidance on cell culture techniques. This research was supported by NUSNNI-Nanocore core fund.

■ REFERENCES

(1) Torre, L. A.; Siegel, R. L.; Jemal, A. Lung cancer statistics. *Adv. Exp. Med. Biol.* **2016**, *893*, 1–19.
(2) Siegel, R. L.; Miller, K. D.; Jemal, A. Cancer statistics. *Ca-Cancer J. Clin.* **2016**, *66*, 7–30.
(3) Cutler, D. M. Are we finally winning the war on cancer? *J. Econ. Perspect.* **2008**, *22*, 3–26.
(4) Amann, A.; de Lacy Costello, B.; Miekisch, W. The human volatilome: volatile organic compounds (VOCs) in exhaled breath, skin emanations, urine, feces and saliva. *J. Breath Res.* **2014**, *8*, 034001.
(5) Broza, YY.; Mochalski, P.; Ruzsanyi, V.; Amann, A.; Haick, H. Hybrid volatolomics and disease detection. *Angew. Chem., Int. Ed.* **2015**, *54*, 11036–11048.
(6) Hakim, M.; Broza, Y. Y.; Barash, O. Volatile organic compounds of lung cancer and possible biochemical pathways. *Chem. Rev.* **2012**, *112*, 5949–5966.
(7) Chung-man, H. J.; Zheng, S.; Comhair, S. A.; Farver, C.; Erzurum, S. C. Differential expression of manganese superoxide dismutase and catalase in lung cancer. *Cancer Res.* **2001**, *23*, 8578–8585.
(8) Pauling, L.; Robinson, A. B.; Teranishi, R.; Cary, P. Quantitative analysis of urine vapor and breath by gas-liquid partition chromatography. *Proc. Natl. Acad. Sci. U. S. A.* **1971**, *68*, 2374–2376.
(9) Moser, B.; Bodrogi, F.; Eibl, G.; Lechner, M.; Rieder, J.; Lirk, P. Mass spectrometric profile of exhaled breath - Field study by PTR-MS. *Respir. Physiol. Neurobiol.* **2005**, *145*, 295–300.
(10) Phillips, M.; Cataneo, RN.; Cummin, A. R. C.; Gagliardi, A. J.; Gleeson, K.; Greenberg, J.; Maxfield, R. A.; Rom, W. N. Detection of lung cancer with volatile markers in the breath. *Chest* **2003**, *123*, 2115–2123.
(11) Bajtarevic, A.; Ager, C.; Pienz, M.; Kliber, M.; Schwarz, K.; Ligor, M.; Ligor, T.; Filipiak, W.; Denz, H.; Fiegl, M.; Hilbe, W.; Lukas, P.; Jamnig, H.; Hackl, M.; Haidenberger, A.; Buszewski, B.; Miekisch, W.; Schubert, J.; Amann, A. Noninvasive detection of lung cancer by analysis of exhaled breath. *BMC Cancer* **2009**, *9*, 348.
(12) Nakhleh, M. K.; Amal, H.; Jeries, R.; et al. Diagnosis and classification of 17 diseases from 1404 subjects *via* pattern analysis of exhaled molecules. *ACS Nano* **2017**, *11*, 112–125.
(13) Filipiak, W.; Mochalski, P.; Filipiak, A.; Ager, C.; Cumeras, R.; Davis, C. E.; Agapiou, A.; Unterkofler, K.; Troppmair, J. A compendium of volatile organic compounds (VOCs) released by human cell lines. *Curr. Med. Chem.* **2016**, *23*, 2112–2131.
(14) Weinberg, R. A. *The Biology of Cancer*, 2nd ed.; Garland Science: New York, 2013; pp 10–25.
(15) Wood, S. L.; Pernemalm, M.; Crosbie, P. A.; Whetton, A. D. Molecular histology of lung cancer: From targets to treatments. *Cancer Treat. Rev.* **2015**, *41*, 361–375.
(16) Peled, N.; Yoshida, K.; Wynes, M. W.; Hirsch, F. R. Review: predictive and prognostic markers for epidermal growth factor receptor inhibitor therapy in non-small cell lung cancer. *Ther. Adv. Med. Oncol.* **2009**, *1*, 137–144.

DOI: 10.1021/acsomega.7b02035
ACS Omega 2018, 3, 5131–5140

(17) Ho, C.; Tong, K. M.; Ramsden, K.; Ionescu, D. N.; Laskin, J. Histologic classification of non-small-cell lung cancer over time: Reducing the rates of not-otherwise-specified. *Curr. Oncol.* **2015**, *22*, 164−170.
(18) Brunner, C.; Szymczak, W.; Höllriegl, V.; et al. Discrimination of cancerous and non-cancerous cell lines by headspace-analysis with PTR-MS. *Anal. Bioanal. Chem.* **2010**, *397*, 2315−2324.
(19) Filipiak, W.; Sponring, A.; Mikoviny, T.; Ager, C.; Schubert, J.; Miekisch, W.; Amann, A.; Troppmair, J. Release of volatile organic compounds from the lung cancer cell line CALU-1 in vitro. *Cancer Cell Int.* **2008**, *8*, 17.
(20) Rutter, A. V.; Chippendale, T. W. E.; Yang, Y.; Španěl, P.; Smith, D.; Sulé-Suso, J. Quantification by SIFT-MS of acetaldehyde released by lung cells in a 3D model. *Analyst* **2013**, *138*, 91−95.
(21) Sponring, A.; Filipiak, W.; Mikoviny, T. Release of volatile organic compounds from the lung cancer cell line NCI-H2087 in vitro. *Anticancer Res.* **2009**, *29*, 419−426.
(22) Davies, M. P. A.; Barash, O.; Jeries, R.; Peled, N.; Ilouze, M.; Hyde, R.; Marcus, M. W.; Field, J. K.; Haick, H. Unique volatolomic signatures of TP53 and KRAS in lung cells. *Br. J. Cancer* **2014**, *111*, 1213−1221.
(23) Peled, N.; Barash, O.; Tisch, U.; Ionescu, R.; Broza, Y. Y.; Ilouze, M.; Mattei, J.; Bunn, P. A., Jr.; Hirsch, F. R.; Haick, H. Volatile fingerprints of cancer specific genetic mutations. *Nanomedicine* **2013**, *9*, 758−766.
(24) Barash, O.; Peled, N.; Tisch, U.; Bunn, P. A.; Hirsch, F. R.; Haick, H. Classification of lung cancer histology by gold nanoparticle sensors. *Nanomedicine* **2012**, *8*, 580−589.
(25) Chen, X.; Xu, F. A Study of the volatile organic compounds exhaled by lung cancer cells in vitro for breath diagnosis. *Cancer* **2007**, *110*, 835−844.
(26) Filipiak, W.; Sponring, A.; Filipiak, A. TD-GC-MS analysis of volatile metabolites of human lung cancer and normal cells in vitro. *Cancer Epidemiol., Biomarkers Prev.* **2010**, *19*, 182−195.
(27) Lavra, L.; Catini, A.; Ulivieri, A.; Capuano, R.; Salehi, L. B.; Sciacchitano, S.; Bartolazzi, A.; Nardis, S.; Paolesse, R.; Martinelli, E.; Di Natale, C. Investigation of VOCs associated with different characteristics of breast cancer cells. *Sci. Rep.* **2015**, *5*, 13246.
(28) Poli, D.; Carbognani, P.; Corradi, M. Exhaled volatile organic compounds in patients with non-small cell lung cancer: cross sectional and nested short-term follow-up study. *Respir. Res.* **2005**, *6*, 71.
(29) Corradi, M.; Poli, D.; Banda, I. Exhaled breath analysis in suspected cases of non-small-cell lung cancer: a cross-sectional study. *J. Breath Res.* **2015**, *9*, 027101.
(30) Ligor, M.; Ligor, T.; Bajtarevic, A. Determination of volatile organic compounds in exhaled breath of patients with lung cancer using solid phase microextraction and gas chromatography mass spectrometry. *Clin. Chem. Lab. Med.* **2009**, *47*, 550−560.
(31) Ayala, A.; Munoz, M. F.; Argüelles, S. Lipid peroxidation: Production, metabolism, and signaling mechanisms of malondialdehyde and 4-hydroxy-2-nonenal. *Oxid. Med. Cell. Longevity* **2014**, *1*, 1−31.
(32) Hakim, M.; Broza, Y. Y.; Barash, O.; Peled, N.; Phillips, M.; Amann, A.; Haick, H. Volatile organic compounds of lung cancer and possible biochemical pathways. *Chem. Rev.* **2012**, *112*, 5949−5966.
(33) Barash, O.; Peled, N.; Hirsch, F. R.; Haick, H. Sniffing the unique odor print of non-small-cell lung cancer with gold nanoparticles. *Small* **2009**, *5*, 2618−2624.
(34) Peng, G.; Tisch, U.; Adams, O. Diagnosing lung cancer in exhaled breath using gold nanoparticles. *Nat. Nanotechnol.* **2009**, *4*, 669−673.
(35) del Nogal Sánchez, M.; García, E. H.; Pavón, J. L. P.; Cordero, B. M. Fast analytical methodology based on mass spectrometry for the determination of volatile biomarkers in saliva. *Anal. Chem.* **2012**, *84*, 379−385.
(36) Warburg, O. On the Origin of Cancer Cells. *Science* **1956**, *123*, 309−314.
(37) Kroemer, G.; Pouyssegur, J. Tumor cell metabolism: cancer's achilles' heel. *Cancer Cell* **2008**, *13*, 472−482.
(38) Krall, A. S.; Xu, S.; Graeber, T. G.; Braas, D.; Christofk, H. R. Asparagine promotes cancer cell proliferation through use as an amino acid exchange factor. *Nat. Commun.* **2016**, *7*, 11457.
(39) Ananieva, E. Targeting amino acid metabolism in cancer growth and anti-tumor immune response. *World J. Biol. Chem.* **2015**, *6*, 281−289.
(40) Tang, Z.; Du, R.; Jiang, S.; Wu, C.; Barkauskas, D. S.; Richey, J.; Molter, J.; Lam, M.; Flask, C.; Gerson, S.; Dowlati, A.; Liu, L.; Lee, Z.; Halmos, B.; Wang, Y.; Kern, J. A.; Ma, P. C. Dual MET−EGFR combinatorial inhibition against T790M-EGFR-mediated erlotinib-resistant lung cancer. *Br. J. Cancer* **2008**, *99*, 911−922.
(41) Currie, E.; Schulze, A.; Zechner, R.; Walther, T. C.; Farese, R. V. Cellular fatty acid metabolism and cancer. *Cell Metab.* **2013**, *18*, 153−161.
(42) Bryant, A.; Cerfolio, R. J. Differences in epidemiology, histology, and survival between cigarette smokers and never-smokers who develop non-small cell lung cancer. *Chest* **2007**, *132*, 185−192.
(43) Barbone, F.; Bovenzi, M.; Cavallieri, F.; Stanta, G. Cigarette smoking and histologic type of lung cancer in men. *Chest* **1997**, *112*, 1474−1479.
(44) Peled, N.; Hakim, M.; Bunn, P. A. Non-invasive breath analysis of pulmonary nodules. *J. Thorac. Oncol.* **2012**, *7*, 1528−1533.
(45) Phillips, C.; Parthaláin, N. M.; Syed, Y.; Deganello, D.; Claypole, T.; Lewis, K. Short-term intra-subject variation in exhaled volatile organic compounds (VOCs) in COPD patients and healthy controls and its effect on disease classification. *Metabolites* **2014**, *4*, 300−318.
(46) Huang, S.-M.; Zuo, X.; Li, J. J.; Li, S. F. Y.; Bay, B. H.; Ong, C. N. Metabolomics studies show dose-dependent toxicity induced by SiO2 nanoparticles in MRC-5 human fetal lung fibroblasts. *Adv. Healthcare Mater.* **2012**, *1*, 779−784.
(47) Zhang, B.; Zhang, H.; Du, C.; Ng, Q. X.; Hu, C.; He, Y.; Ong, C. N. Metabolic responses of the growing Daphnia similis to chronic AgNPs exposure as revealed by GC-Q-TOF/MS and LC-Q-TOF/MS. *Water Res.* **2017**, *114*, 135−143.

DOI: 10.1021/acsomega.7b02035
ACS Omega 2018, 3, 5131−5140